Ceramics International xxx (xxxx) xxx

Contents lists available at ScienceDirect

Ceramics International

journal homepage: www.elsevier.com/locate/ceramint

# Glass-based composites comprised of $CaWO_4$:$Yb^{3+}$, $Tm^{3+}$ crystals and $SrAl_2O_4$:$Eu^{2+}$, $Dy^{3+}$ phosphors for green afterglow after NIR charging

E. Santos Magalhães [a,*], A. Sedda [a,b], B. Bondzior [a,c], S. Vuori [d,e], D. Van der Heggen [f], P.F. Smet [f], M. Lastusaari [d], L. Petit [a,*]

[a] Photonics Laboratory, Tampere University, Korkeakoulunkatu 3, Tampere 33720, Finland
[b] Department of Physics, LUT-University, Lappeenranta, Finland
[c] Institute of Low Temperature and Structure Research PAS, Okolna 2, 50-422 Wrocław, Poland
[d] Department of Chemistry, University of Turku, FI-20014 Turku, Finland
[e] University of Turku Graduate School (UTUGS), Doctoral Programme in Exact Sciences, Turku, Finland
[f] LumiLab, Department of Solid State Sciences, Ghent University, Krijgslaan 281-S1, 9000 Gent, Belgium

ARTICLE INFO

Handling Editor: Dr P. Vincenzini

ABSTRACT

In this paper, we demonstrated the fabrication of new phosphate-based composites with green persistent luminescence after being charged with near-infrared light using the direct doping method. The composites are composed of a phosphate glass and phosphors. The $75NaPO_3 - 25CaF_2$ and $90NaPO_3 - 10NaF$ (in mol%) were the 2 glasses of investigation. The intense blue up-conversion emission between 450 and 500 nm upon 980 nm pumping is obtained by adding $CaWO_4$: $Tm^{3+}$, $Yb^{3+}$ crystals in the glass melt before quenching whereas the green persistent luminescence is from the $SrAl_2O_4$:$Eu^{2+}$,$Dy^{3+}$ phosphors also added in the glass melt. The green persistent luminescence above 0.3 mcd/$m^2$ is observed for ~30 min after charging with 980 nm due to energy transfer between the upconverter crystals and the persistent luminescent phosphors. Here, the challenges related to the fabrication of such composites are discussed. While it is important for the blue UC emission to be intense to charge the $SrAl_2O_4$:$Eu^{2+}$,$Dy^{3+}$ crystals, we demonstrate that the glass matrix should not crystallize upon the addition of the different crystals. Additionally, the composites should remain translucent with limited light scattering for the blue UC emission to charge the persistent luminescent phosphors.

## 1. Introduction

Persistent luminescent materials have been of great importance as they can emit light for hours once the excitation source, responsible for charging it, is removed [1]. Such materials have found uses in emergency signalization, thermal sensors and bioimaging [2–4]. This persistent luminescence, also called afterglow, is a consequence of energy storage in the material during excitation. The absorption of the excitation light induces a charge transfer process which finally leads to charge trapping at defect sites. The spontaneous release of the trapped charges at room temperature leads to the delayed emission of a photon after recombination [5].

Since the discovery of the first so-called modern PeL phosphor $SrAl_2O_4$:$Eu^{2+}$,$Dy^{3+}$ [6,7], efforts have been focused on developing new PeL materials, including PeL glasses [8,9]. Such PeL glasses have been prepared by adding the PeL phosphors in the glass melt. However, dissolution of the phosphors was reported to occur during the glass preparation leading to degradation in the PeL properties [10]. The degree of dissolution was found to depend not only on the temperature of the melt but also on the glass composition [11]. When the $SrAl_2O_4$:$Eu^{2+}$, $Dy^{3+}$ PeL phosphors are added in passive glass matrix, green afterglow can only be obtained when the material is exposed to UV, blue or even white light. Recently, we demonstrated that if the $SrAl_2O_4$:$Eu^{2+}$,$Dy^{3+}$ particles are added in $Yb^{3+}$, $Tm^{3+}$ codoped oxyfluorophosphate glass [12], green afterglow can be seen after 980 nm illumination. This is achieved due to an upconversion process using $Yb^{3+}$ and $Tm^{3+}$ ion pair: the NIR photons are absorbed by $Yb^{3+}$ which, then, populate $Tm^{3+}$ energy levels via an energy transfer mechanism. This process leads to an emission of UV/blue light which can be used to charge the $SrAl_2O_4$:$Eu^{2+}$, $Dy^{3+}$ as in Ref. [13].

It is well known that the spectroscopic properties of rare-earth (RE) ions can be greatly enhanced if the RE are embedded in crystal with

* Corresponding authors.
*E-mail addresses:* evellyn.santosmagalhaes@tuni.fi (E. Santos Magalhães), laeticia.petit@tuni.fi (L. Petit).

https://doi.org/10.1016/j.ceramint.2023.01.155
Received 19 December 2022; Received in revised form 18 January 2023; Accepted 19 January 2023
Available online 20 January 2023

specific crystalline phase [14]. Additionally, the most efficient upconversion media are crystals with low phonon energy, as the low phonon energy of the host decreases the rate of nonradiative multiphonon relaxation from upper levels, leading to high efficiency of the up-conversion process [15]. Thus, efforts have been focused on RE doped fluoride crystals due to their low phonon energy and thus high UC efficiency. Among various fluoride crystals, $NaYF_4$ crystals have been considered the most efficient UC materials [16,17]. Upconverter glasses were successfully prepared by adding $Er^{3+}$, $Yb^{3+}$ codoped $NaYF_4$ crystals in the $90NaPO_3$–10NaF (in mol%) glass melt at 550 °C prior to casting the glass [18]. However, the evaporation temperature of the $NaYF_4$ crystals is low (750 °C) [19] limiting the number of glasses in which such crystals can be embedded. For example, the $NaYF_4$ crystals completely decompose when added in the glass melt of the $75NaPO_3$–$25CaF_2$ (in mol%) glass due to the high melting temperature (>950 °C). $CaWO_4$ is another efficient luminescent host due its low phonon threshold energy [20]. Recent studies showed that solid-state method can be used to synthesize $Tm^{3+}$, $Yb^{3+}$ codoped $CaWO_4$ crystals with structures of the scheelite oxide type, uniform morphology and blue upconversion under 980 nm pumping [21].

Herein, we present an alternative approach to prepare NIR rechargeable glass-based materials with green persistent luminescence by adding $Tm^{3+}$, $Yb^{3+}$ codoped $CaWO_4$ crystals and $SrAl_2O_4$: $Eu^{2+}$,$Dy^{3+}$ phosphors in phosphate glasses with the composition $90NaPO_3$–10NaF and $75NaPO_3$–$25CaF_2$ (in mol%). These glasses were selected due to their different melting temperature.

## 2. Experimental

$CaWO_4$: $Yb^{3+}$, $Tm^{3+}$ crystals were prepared via solid-state reaction with 0.5 mol% of $Tm_2O_3$ and the $Yb_2O_3$ content ranging from 5 to 25 mol% as in Ref. [22]. The trivalent dopants substituting divalent host ions $Ca^{2+}$ were compensated for charge with monovalent $Na^+$ with equal percentage as both trivalent dopants as in Ref. [23]. The raw chemicals were $CaCO_3$ (Alfa-Aesar, technical grade), $WO_3$ (Honeywell-Fluka, 99%),$Yb_2O_3$ (Sigma-Aldrich, 99,9%), $Tm_2O_3$(Honeywell, ≥99%) and $Na_2CO_3$ (Sigma-Aldrich, 99,9%). The chemicals were mixed and heated to 1200 °C using a 3 °C/min heating rate in ambient atmosphere. The duration of the thermal treatment was 4 h. Crystals were prepared with different amount of $Yb_2O_3$ (from 5 to 25 mol%) and 0.5 mol % of $Tm_2O_3$. They are labeled as YbxTm0.5.

Phosphate glasses with the composition (in mol%) $75NaPO_3$ − $25CaF_2$ (labeled as Ca glasses) and $90NaPO_3$ − 10NaF (labeled as Na glasses) were prepared with different amount of $CaWO_4$:$Tm^{3+}$, $Yb^{3+}$ (0, 2.5, 5 and 7.5 wt%) and of $SrAl_2O_4$:$Eu^{2+}$, $Dy^{3+}$ (Realglow®) (1 and 2 wt %). $NaPO_3$ (Alfa Aesar, *tech.*), NaF (Sigma-Aldrich, *99.99%*) and $CaF_2$ (Honeywell-Fluka, 99%) were used as the raw materials. The Na glasses were melted in quartz crucible at 750 °C whereas the Ca glasses were melting in Pt crucible at 950 °C. All melting were performed in ambient atmosphere. The $CaWO_4$:$Tm^{3+}$, $Yb^{3+}$ and $SrAl_2O_4$:$Eu^{2+}$, $Dy^{3+}$ were added in the glass melt after the melting and prior to quenching. After quenching, the glasses were annealed at 40 °C below their respective glass transition temperature for 5 h to release the stress from the quench. The Na and Ca composites are labeled according to their $CaWO_4$ - PeL wt %.

NETZSCH STA 449 F1 Differential Scanning Calorimeter (DSC) was used to measure the thermal properties of the glasses. The heating rate was 10 °C/min. The glass transition temperature ($T_g$) was taken as the inflection point of the first endothermic signal. The crystallization temperature ($T_p$) corresponds to the exothermic peak maximum and the onset of crystallization ($T_x$) to the intersection of the tangent of the exotherm peak with the baseline.

Scanning Electron Microscopy (SEM) (Crossbeam 540, Carl Zeiss, Oberkochen, Germany) with an EDS detector (X-MaxN 80, Oxford Instruments, Abingdon-on-Thames, UK) were used to image and analyze the composition of the samples which were coated with a conductive carbon layer to reduce charging of the samples.

The XRD patterns of the crystals and of the composites were measured using PANalytical EMPYREAN multipurpose X-ray diffractometer (PANalytical, Almelo, The Netherlands). A Ni filtered Cu-Kα radiation was used and the diffractograms were measured from $2\theta = 15°–80°$ with a step of 0.013°. The Na and Ca composites were crushed into powder prior to the measurement.

The transmission spectra of the Na and Ca glasses and composites were measured using polished samples from a range of 200 nm–600 nm. The spectra were obtained using a UV-VIS-Near-IR Spectrophotometer (UV-3600 Plus, Shimadzu). The reflectance measurements were conducted with Avantes AvaSpec HS-TEC using Avantes AvaLight-DHc as the light source. 1000 μm VIS/NIR 0.37NA PC04 fibers were connected to the spectrometer and the light source. The white reference was MgO powder. The detector's integration time was kept at 500 m s with 5 averages per measurement.

The upconversion (UC) spectra of the composites, crushed into powder, were recorded using a TEC-cooled fiber-coupled multimode laser (II-VI Laser enterprise), with $\lambda_{exc} = 980$ nm, 1 A. The emission spectra were measured in a range of 400–700 nm by means of a Spectro 320 optical spectrum analyzer (Instrument Systems Optische Messtechnik GmbH, Germany). The measurements were obtained at room temperature and on glass powder to allow the comparison of the UC intensity.

The PeL spectra of the samples were acquired with a Varian Cary Eclipse Fluorescence Spectrophotometer equipped with a Hamamatsu R928 photomultiplier tube (PMT). The measurements were performed at room temperature. The samples, crushed into powder to allow the comparison of the PeL intensity between the composites, were irradiated for 5 with a hand-held 254 nm UV lamp (UVGL-25, 4 W) after which the PeL spectra were collected 1 min after stopping the irradiation. The detector parameters were: Bio-/chemiluminescence mode, scan range 400–1000 nm, emission slit 20 nm, data interval 1.0000 nm, PMT voltage 600 V (medium).

The PeL decay curve measurements were conducted by irradiating the powdered sample for 5 min with a 254 nm hand-held UV-lamp (UVGL-25), after which the luminance values were obtained by taking a measurement every second starting 1 s after stopping the irradiation. The equipment consisted of Hagner ERP-105 luminance meter coupled with a Hagner SD 27 detector. The PeL decay after illumination with a 980 nm laser (200 mW) focused on 0.25 $mm^2$, was recorded using an ILT 1700 calibrated photometer (International Light Technologies) equipped with a photopic filter (YPM). For these measurements a thick metal plate with a circular hole (Ø 5 mm) was inserted between the sample (bulk form) and the detector in an attempt to exclude effects due to differences in the sample's lateral size and morphology.

## 3. Results and discussion

$CaWO_4$ crystals were prepared with 0.5 mol% of $Tm_2O_3$ and the $Yb_2O_3$ content ranging from 5 to 25 mol% in order to optimize the $Tm^{3+}/Yb^{3+}$ ratio. The XRD pattern of the crystals are presented in Fig. 1a. The XRD patterns of the as-prepared crystals exhibit peaks, the position of which corresponds well to those of standard Powder Diffraction File entry 04-008-6874 of $CaWO_4$, confirming that the rare earth dopant ions substitute $Ca^{2+}$, due to similar ionic radii – 112 p.m. for $Ca^{2+}$, 99.4 p.m. for $Tm^{3+}$, 98.5 p.m. for $Yb^{3+}$ [24] and 118 p.m. for $Na^+$ (all values of ionic radii are given for 8-coordinated ions, as present in $CaWO_4$ [25]). The XRD peaks shift towards higher angles with an increase in the $Yb_2O_3$ content suggesting a contraction of the structure due to the different ionic radii. The successful charge compensation with $Na^+$ is also indicated by the lack of any secondary phases. The morphology and size of the crystals were characterized using SEM. As depicted in Fig. 1b, the crystals are small granules with various shapes and their size ranges from ~10 μm to 30 μm, independently of the rare-earth content.

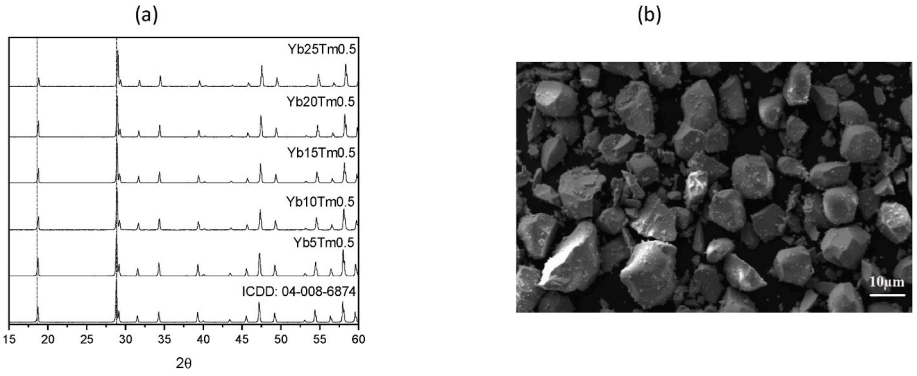


**Fig. 1.** (a) XRD pattern of the $CaWO_4$ crystals prepared with different amount of $Yb_2O_3$ and 0.5 mol% of $Tm_2O_3$. (b) SEM image of the $CaWO_4$ crystal prepared with 15 mol% of $Yb_2O_3$ and 0.5 mol% of $Tm_2O_3$.

The crystals emit blue light under 980 nm excitation which could be seen with naked eyes. The UC spectrum of the crystal, Yb15Tm0.5 taken as an example is shown in Fig. 2a. All the investigated crystals, independently of the RE content, exhibit the same UC spectrum. The UC spectra exhibit 3 main bands which are typical of the emission from $Tm^{3+}$ ions: the bands at 450, 475 and 650 nm corresponds to the $^1D_2 \rightarrow {}^3F_4$, $^1G_4 \rightarrow {}^3H_6$ and $^1G_4 \rightarrow {}^3F_4$ transitions of $Tm^{3+}$, respectively. The intensity of the emission centered at 650 nm is weaker than that of the emission centered at 475 nm. Similar results were reported in Ref. [26]. The progressive addition of $Yb_2O_3$ up to 15–20 mol% increases the intensity of the blue emission at 475 nm (Fig. 2b) confirming the role of $Yb^{3+}$ ions as sensitizers. However, for larger amount of $Yb_2O_3$ (>25 mol %), the intensity of the blue emission decreases due to concentration quenching. One should point out that the concentration quenching was reported to occur already at 5 mol% of $Yb_2O_3$ in $CaWO_4$ crystals when prepared with 1 mol% of $Tm_2O_3$ [26].

Composites were prepared by adding 1.25 to 7.5 wt% of $CaWO_4$ crystals (UC crystals) prepared with 0.5 mol% of $Tm_2O_3$ and 15 mol% of $Yb_2O_3$ and 1 wt% of $SrAl_2O_4$:$Eu^{2+}$, $Dy^{3+}$ PeL phosphors in glass melt prior to quenching. Fig. 3a and b shows the picture in daylight and after stopping the UV of the Ca and Na composites, respectively. While the Na composites remain glassy after adding the UC crystals and the PeL phosphors, the Ca composites are opaque, especially when prepared with a large amount of the UC crystals. The opacity can be related to the crystallization of the glass matrix as evidenced in Fig. 4a which presents the XRD pattern of the Na and Ca composites prepared with 7.5 wt% of $CaWO_4$ crystals and 1 wt% of PeL particles. The XRD pattern of the two composites exhibits the peaks which correspond to those of the $CaWO_4$ crystals [04-008-6874]. No XRD peaks related to the PeL particles could be seen due to their low amount of in the glass matrices. Additional peaks, represented with *, can be seen especially in the XRD pattern of the Ca composites confirming the presence of additional crystalline phase in large amount in the Ca glass matrix. However, the peaks are too few and in too low intensity to identify the crystalline phase. The crystallization of the Ca composites when adding various crystals in the glass melt might be related to the thermal properties of the Ca glass. As shown in Table 1, the Na glass can be considered as a stable glass against crystallization based on its large $\Delta T$ ($T_x$-$T_g$). However, the $\Delta T$ ($T_x$-$T_g$) of the Ca glass is ~43 °C revealing the poor resistance of this glass against crystallization. The UC crystals and PeL phosphors are thus expected to act as nucleation agent when added in the Ca glass melt.

The loss in transmittance after adding the crystals and PeL particles is evidenced in Fig. 4b and c. As suspected from Fig. 3, the Na composites are more transparent than the Ca composites when prepared with similar amount of crystals and PeL particles.

As shown in Fig. 3, all the composites exhibit green afterglow after stopping UV confirming the survival of the PeL particles during the composites preparation as discussed in Refs. [10,11]. Homogeneous afterglow can be seen from the composites revealing homogeneous dispersion of the PeL particles in the glass matrices. Independently of the amount of the UC crystals and of the glass composition, all the composites exhibit similar PeL emission band which is due to $4f^6 5\,d^1 \rightarrow 4f^7$ transition of $Eu^{2+}$ (Fig. 5a) [27,28]. However, the composites exhibit different intensity of the green PeL as depicted in Fig. 5b. Also shown in Fig. 5b is the green PeL intensity of References (Ref), $NaPO_3$ powder mixed with the same amount of $CaWO_4$ and PeL particles than those in the composites. While the Na composites exhibit similar intensity of green PeL than the references, weaker PeL is collected from the Ca composites probably due to their poor transmittance properties. As suggested in Refs. [10,11], it is possible that PeL particles also decompose during the preparation of the Ca composite due to the high melting temperature used to melt the Ca glass (950 °C). It is interesting to point

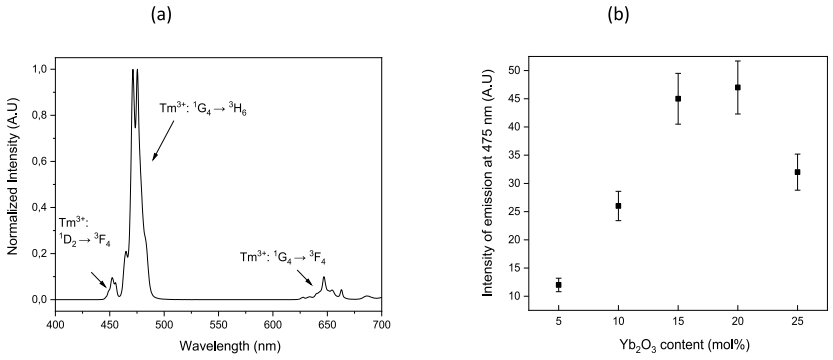


**Fig. 2.** (a) Normalized upconversion spectrum of the Yb15Tm0.5 crystal, taken as an example ($\lambda_{exc}$ = 980 nm) and (b) relative intensity of the blue emission at 450 nm as a function of the $Yb_2O_3$ mol% in the crystals ($\lambda_{exc}$ = 980 nm).

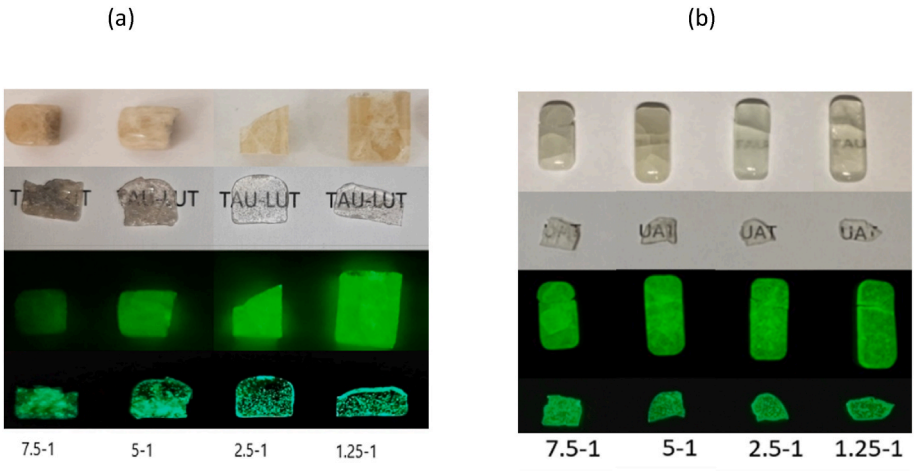


**Fig. 3.** Picture in daylight (top) and after stopping UV (bottom) of the Ca (a) and Na (b) composites prepared with different wt% of $CaWO_4$ (from 7.5 to 1.25) and 1 wt% of PeL $SrAl_2O_4:Eu^{2+}$, $Dy^{3+}$ particles.

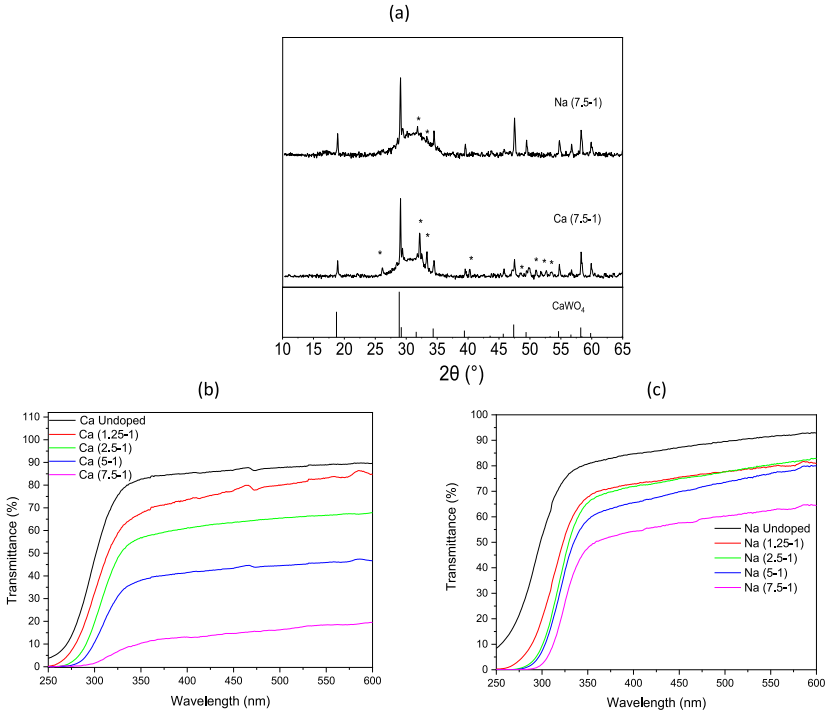


**Fig. 4.** (a) XRD pattern of the Na and Ca composites prepared with 7.5 wt% of CaWO4 and 1 wt% of PeL $SrAl_2O_4:Eu^{2+}$, $Dy^{3+}$ particles. Also shown are the reference data for $CaWO_4$ crystals [04-008-6874]. Transmittance spectra of the Ca (b) and Na (c) composites with different wt% of $CaWO_4$ (from 1.25 to 7.5) and 1 wt% of $SrAl_2O_4:Eu^{2+}$, $Dy^{3+}$ PeL particles (thickness of 1 mm).

**Table 1**
Thermal properties of the Na and Ca glasses prepared with no crystals nor PeL particles.

| | $T_g \pm 3$ (°C) | $T_x \pm 3$ (°C) | $\Delta T$ ($T_x$-$T_g$) ± 6 (°C) | $T_p \pm 3$ (°C) |
|---|---|---|---|---|
| Na glass | 266 | 358 | 92 | 404 |
| Ca glass | 277 | 320 | 43 | 332 |

out that an increase in the content of the $CaWO_4$ crystals from 1.25 to 2.5 wt% increases slightly the intensity of the PeL probably due to the fact that under 266 nm charging, the UC crystals emit blue emission [29] charging the PeL phosphors. However, as the concentration of the UC crystals increases from 2.5 to 7.5 wt%, a slight decrease in the intensity of the green PeL is observed. It is the decrease in the transmittance of the glasses with the progressive incorporation of the UC crystals which is thought to lead to less efficient UV charging and so to PeL with low intensity. Another probable explanation to the afterglow reduction is the self-absorption of the glass, occurring especially in the Ca glasses. The reflectance spectra of the samples measured from powder are depicted in Fig. 6. One should point out that the reflectance spectra were collected from composites crushed into powder and cannot be related to the transmittance spectra presented in Fig. 4b and c. Nonetheless, from the reflectance spectra, it is shown that the amount of absorbed light increases with an increase in the wt% of the UC crystals. While the reflectance spectra of the Ca(1.25–1) and Ca(2.5–1) samples are almost on the same level, the Ca(5–1) and Ca(7.5–1) composites show increased

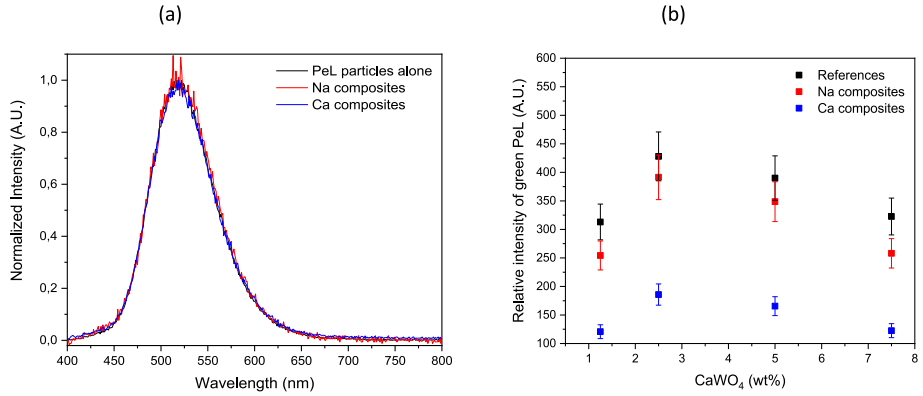


**Fig. 5.** – (a) Normalized PeL spectra of the Ca and Na composites prepared with 7.5 wt% of $CaWO_4$ and 1 wt% of $SrAl_2O_4:Eu^{2+}$, $Dy^{3+}$ PeL particles taken as examples. Also shown in the normalized PeL spectrum of the PeL particles alone ($\lambda_{exc} = 266$ nm). (b) PeL intensity of the Ca and Na composites prepared with 1 wt% of PeL and different amount of $CaWO_4$ crystals.

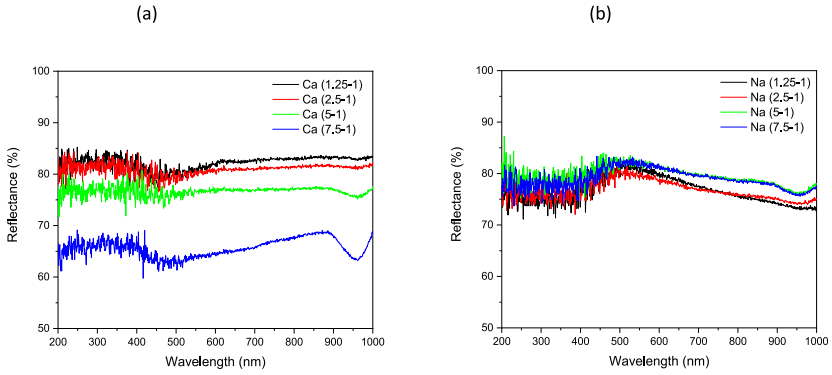


**Fig. 6.** Reflectance spectra of the Ca (a) and Na (b) composites, crushed into powder and prepared with different wt% of $CaWO_4$ (from 1.25 to 7.5) and 1 wt% of $SrAl_2O_4:Eu^{2+}$, $Dy^{3+}$ PeL particles.

absorption throughout the whole visible spectrum. These observations are in agreement with Fig. 3a, where it can be seen that the samples are increasingly darker when a large amount of UC crystals is added to the glass matrix.

The normalized UC spectra of the Na and Ca composites prepared with 5 wt% of $CaWO_4$ and 1 wt% of PeL $SrAl_2O_4:Eu^{2+}$, $Dy^{3+}$ particles, taken as examples as all the composites exhibit the same shape of UC emission bands, are presented in Fig. 7a. Under 980 nm pumping, the spectra exhibit the same 3 emission bands located at 450, 475 and 650 nm as those seen in the UC spectra of the as-prepared UC crystals (Fig. 2a) revealing that the UC crystals also survive the melting process. As expected, an increase in the wt% of the UC crystals increases the intensity of the visible emission from 400 to 700 nm. However, as shown in Fig. 7b, the Na and Ca composites exhibit lower intensity of the blue emission at 475 nm than the References suggesting that some $CaWO_4$ crystals decompose in the glass melt during the preparation of the composites as observed when adding crystals in glass melts [10,11]. As for their afterglow properties, the Na composites exhibit more intense

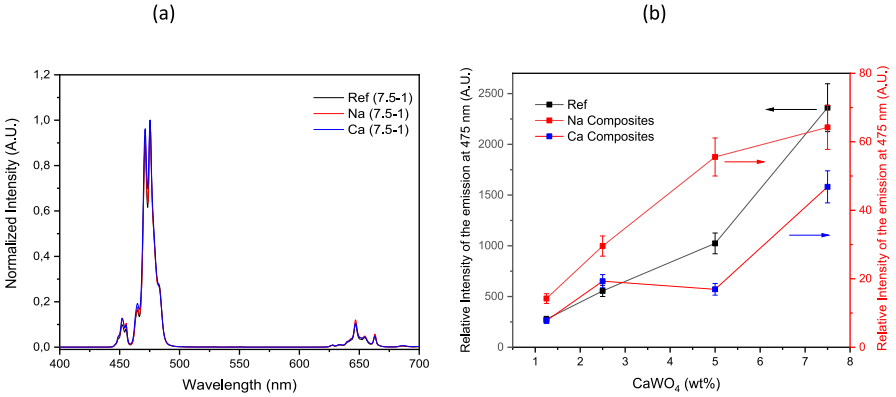


**Fig. 7.** (a) Normalized upconversion of reference, Na and Ca composites prepared with 2.5 wt% of $CaWO_4$ and 1 wt% of $SrAl_2O_4:Eu^{2+}$, $Dy^{3+}$ PeL particles, (b) Intensity of the blue emission from reference, Na and Ca composites prepared with 1 wt% of PeL phosphors as a function of $CaWO_4$ wt%. (For interpretation of the references to color in this figure legend, the reader is referred to the Web version of this article.)

blue light than the Ca composites, probably due to the self-absorption effects caused by the body color of the glass and their lower melting temperature which limits the decomposition of the UC crystals during the glass preparation.

When charged with 254 nm (6 mW/cm$^2$ irradiance) for 5 min, all the Na and Ca composites emit green light above the 0.3 mcd/m$^2$ (the limit set in the exit signage standards [30] as the practical limit of visibility) for 45 and 35 min, respectively which is shorter than the 88 min observed from the Reference samples (Fig. 8a and b). This difference in decay time is due to the decomposition of the crystals and PeL particles during the glass melting and to the less efficient UV charging due to transmittance properties of the composites as already discussed. When charged with 980 nm for 5 min, the composites emit, also, green light due to the overlap between the UC emission (especially between 450 and 500 nm) and the thermoluminescence excitation spectrum of the PeL particles [31]. The intensity of the green afterglow and decay time to 0.3 mcd/m$^2$ (Table 2) is found to decrease with an increase in the concentration of the UC crystals, probably due to the scattering of the 980 nm which leads to less efficient charging of the PeL particles. It is also possible that the distance the blue light has to travel to the PeL phosphors is longer when incorporating a larger amount of UC crystals due to scattering. The decrease in the green afterglow for higher concentration of UC crystals might be also related to an increase in temperature caused by the 980 nm laser during charging which induces thermal detrapping or by stimulated light emission (optically stimulated luminescence) from the PeL phosphors [32]. Since the IR laser used to excite the glasses is focussed in a small spot to efficiently generate the UC-emission, the low decay time for Na(1.25–1) is probably due to the low concentration of UC crystals in the tested area indicating that a compromise should be set between the amount of UC and transmittance properties of the composites. As listed in Table 2, the Na composites prepared with 2.5 and 5 wt% of UC crystals have an afterglow decay time of 30 min which is longer than the 14 min afterglow decay time reported for the $Yb^{3+}$,$Tm^{3+}$ codoped oxyfluorophosphate glass-based composite (labeled as Yb3Tm0.05) reported in Ref. [12]. However, the Yb3Tm0.05 composite was prepared with 2 wt% of PeL phosphors. As shown in Fig. 9a, an increase in the amount of PeL phosphors reduces the intensity of the UC emission probably due to scattering as mentioned already, leading to less efficient pumping.

**Table 2**
Time (min) to reach 0.3 mcd/m$^2$ after 980 nm charging for 2 min the Na and Ca composites prepared with 1 wt% of PeL phosphors and various wt% of Concentration of $CaWO_4$.

| | Concentration of $CaWO_4$ (wt%) | | | |
|---|---|---|---|---|
| | 1.25 | 2.5 | 5 | 7.5 |
| Na composites | (2 ± 1) min | (~30 ± 1) min | (29 ± 1) min | (2 ± 1) min |
| Ca composites | (11 ± 1) min | (6 ± 1) min | (5 ± 1) min | (3 ± 1) min |

Thus, in order to compare the PeL properties after NIR charging of the new composites to those reported in Ref. [12], the Na and Ca composites were prepared with 2 wt% of PeL phosphors as in Ref. [12]. The concentration of the UC crystals was reduced to 1.25 wt% in the Ca composites to reduce the risk of crystallizing the glass matrix when adding larger amount of PeL phosphors. The composites exhibit homogeneous and strong green PeL (Fig. 9b). The Na composite exhibits the most intense blue UC whereas similar intensity of the blue UC was observed from the Ca composite and Yb3Tm0.05 (Fig. 9c). As shown in Fig. 9d, the Ca composite exhibits higher PeL after NIR charging than Yb3Tm0.05 and reaches 0.3 mcd/m$^2$ after 980 nm charging for 2 min after more than 30 min, which is longer than the reported 14 min from the Yb3Tm0.05, indicating that embedding crystals with blue upconversion in glass matrix is promising for the preparation of NIR rechargeable composite with green afterglow. However, one should point out that the intensity of the PeL from the Na composite is lower than expected from Fig. 8d probably due to the different sample morphology (including roughness) and dimensions of the sample, clearly showing that it is crucial, in the future studies, to prepare

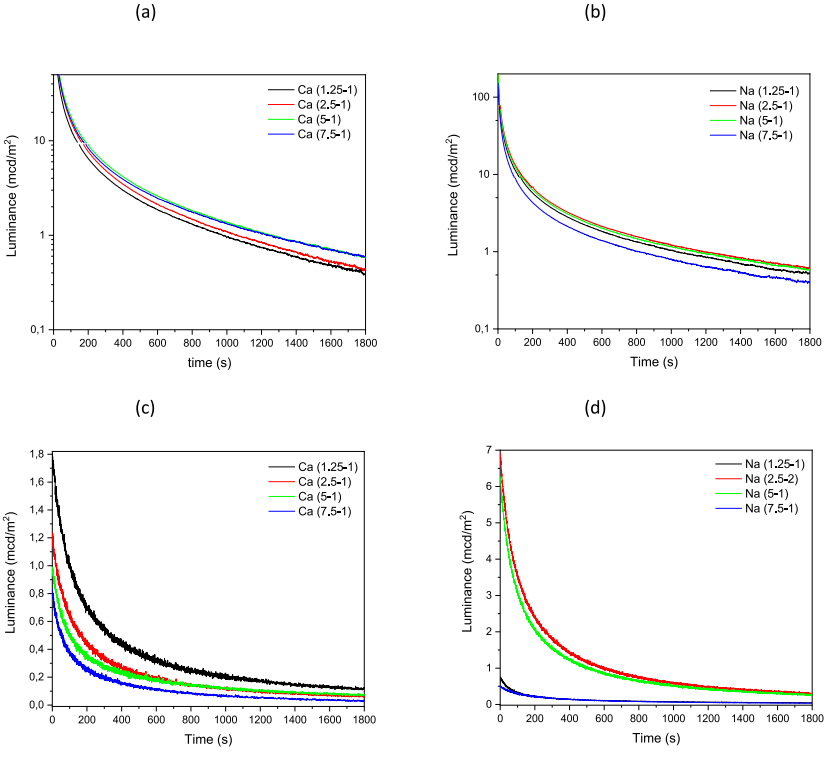


**Fig. 8.** Decay curves obtained from the Ca composites (a and c) and Na composites (b and d) prepared with different amount of $CaWO_4$ and 1 wt% of $SrAl_2O_4$:$Eu^{2+}$, $Dy^{3+}$ PeL particles after 254 and 980 nm charging, respectively.

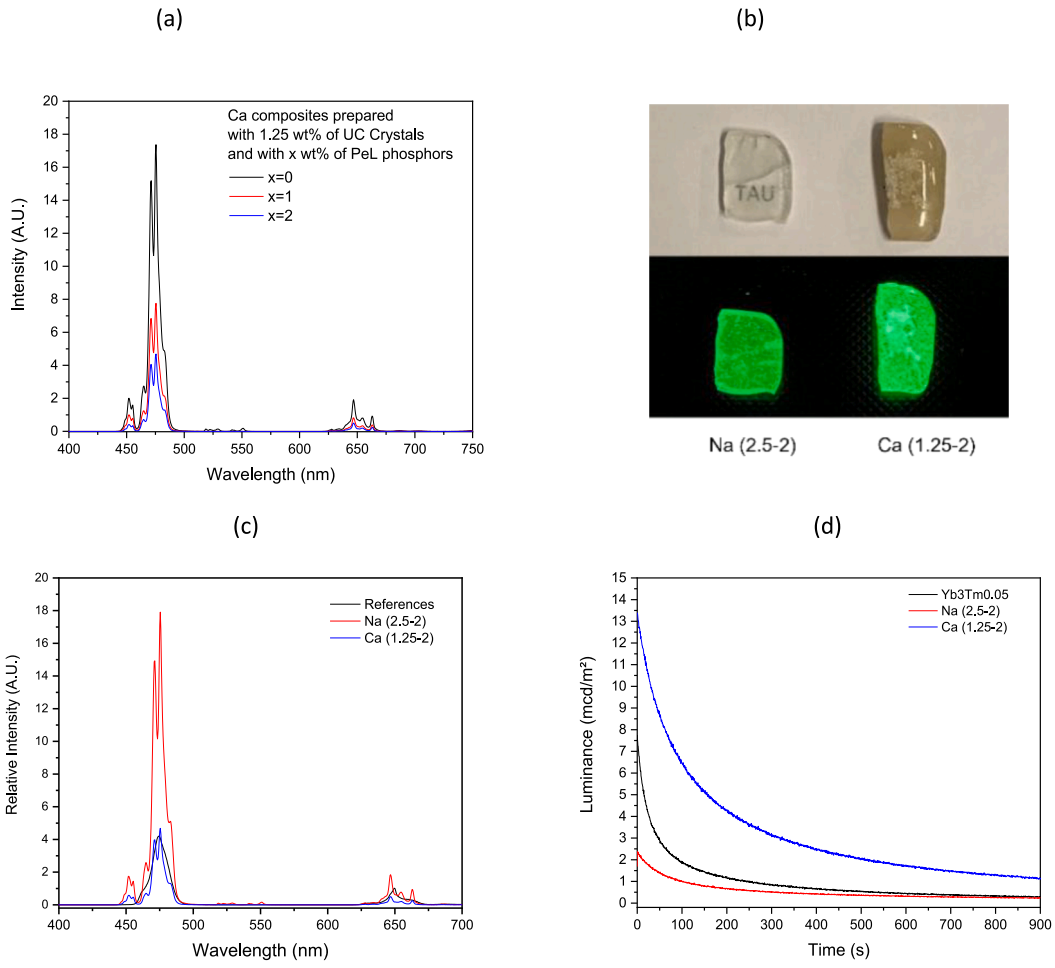


**Fig. 9.** (a) Upconversion spectra of the Ca composites prepared 0, 1 and 2 wt% of PeL phosphors and 1.25 wt% of UC crystals, taken as an example. All UC spectra were measured using $\lambda_{exc} = 980$ nm; (b) Picture in daylight (top) and after stopping UV (bottom) of the Ca and Na composites prepared with 2 wt% of PeL phosphors and 2.5 and 1.25 wt% of $CaWO_4$, respectively; (c) Upconversion spectra of the Yb3Tm0.05 from Ref. [12], Ca and Na composites with 2 wt% of PeL phosphors and 1.25 and 2.5 wt% of $CaWO_4$, respectively; (d) Decay curves obtained from Yb3Tm0.05 from Ref. [12], Ca and Na composites with 2 wt% of PeL phosphors and 1.25 and 2.5 wt% of $CaWO_4$, respectively after 980 nm charging.

composites not only with similar transmittance properties but also with similar dimension and surface quality to allow for an absolute comparison of their PeL performances after NIR charging.

## 4. Conclusion

In summary, we demonstrated that phosphate glass-based composites with green afterglow after NIR charging can be prepared using direct doping method. Here, $CaWO_4$:$Tm^{3+}$, $Yb^{3+}$ crystals were prepared by solid-state reaction. For intense blue UC emission upon 980 nm excitation, the concentration of $Yb_2O_3$ and $Tm_2O_3$ in the $CaWO_4$ should be ~15 mol% and 0.5 mol%, respectively. These crystals were added at the same time as the $SrAl_2O_4$:$Eu^{2+}$,$Dy^{3+}$ particles in the glass melt prior to the quenching step. We showed that the concentration of the upconverter crystals should be tailored so that the blue emission is intense, while keeping high transparency of the composites. The glass matrix should be chosen accordingly as no crystallization should occur upon the addition of the $CaWO_4$:$Tm^{3+}$, $Yb^{3+}$ crystals and $SrAl_2O_4$:$Eu^{2+}$, $Dy^{3+}$ particles into the glass matrix, in order to limit light scattering which is detrimental to the charging of the $SrAl_2O_4$:$Eu^{2+}$,$Dy^{3+}$ particles. After excitation with 980 nm, the afterglow intensity of the newly developed scaffolds with optimized composition remains for ~30 min above the threshold level of 0.3 mcd/$m^2$.

## Declaration of competing interest

The authors declare that they have no known competing financial interests or personal relationships that could have appeared to influence the work reported in this paper.

## Acknowledgements

This work was supported by Academy of Finland [Flagship Programme, Photonics Research and Innovation PREIN-320165] and the Fund for Scientific Research–Flanders (FWOVlaanderen) [research project G0F9322N]. -

## References

[1] T. Aitasalo, J. Hölsä, H. Jungner, M. Lastusaari, J. Niittykoski, Thermoluminescence study of persistent luminescence materials: $Eu^{2+}$- and $r^{3+}$-doped calcium aluminates, $CaAl_2O_4$:$Eu^{2+}$, $R^{3+}$, J. Phys. Chem. B 110 (2006) 4589–4598, https://doi.org/10.1021/jp057185m.

[2] Q. le Masne de Chermont, C. Chanéac, J. Seguin, F. Pellé, S. Maîtrejean, J.-P. Jolivet, D. Gourier, M. Bessodes, D. Scherman, Nanoprobes with near-infrared persistent luminescence for in vivo imaging, Proc. Natl. Acad. Sci. U.S.A. 104 (2007) 9266–9271, https://doi.org/10.1073/pnas.0702427104.

[3] D. Poelman, D. Van der Heggen, J. Du, E. Cosaert, P.F. Smet, Persistent phosphors for the future: fit for the right application, J. Appl. Phys. 128 (2020), 240903, https://doi.org/10.1063/5.0032972.

[4] J. Xu, S. Tanabe, Persistent luminescence instead of phosphorescence: history, mechanism, and perspective, J. Lumin. 205 (2019) 581–620, https://doi.org/10.1016/j.jlumin.2018.09.047.
[5] H.F. Brito, J. Hölsä, T. Laamanen, M. Lastusaari, M. Malkamäki, L.C.V. Rodrigues, Persistent luminescence mechanisms: human imagination at work, Opt. Mater. Express 2 (2012) 371–381, https://doi.org/10.1364/OME.2.000371.
[6] T. Matsuzawa, Y. Aoki, N. Takeuchi, Y. Murayama, A new long phosphorescent phosphor with high brightness, $SrAl_2O_4$ : $Eu^{2+}$ , $Dy^{3+}$, J. Electrochem. Soc. 143 (1996) 2670, https://doi.org/10.1149/1.1837067.
[7] D. Van der Heggen, J.J. Joos, A. Feng, V. Fritz, T. Delgado, N. Gartmann, B. Walfort, D. Rytz, H. Hagemann, D. Poelman, B. Viana, P.F. Smet, Persistent luminescence in strontium aluminate: a roadmap to a brighter future, Adv. Funct. Mater. (2022), 2208809, https://doi.org/10.1002/adfm.202208809.
[8] J. Massera, M. Gaussiran, P. Gluchowski, M. Lastusaari, L. Hupa, L. Petit, Processing and characterization of phosphate glasses containing $CaAl_2O_4$:$Eu^{2+}$, $Nd^{3+}$ and $SrAl_2O_4$:$Eu^{2+}$, $Dy^{3+}$ microparticles, J. Eur. Ceram. Soc. 35 (2015) 3863–3871, https://doi.org/10.1016/j.jeurceramsoc.2015.06.031.
[9] T. Nakanishi, S. Tanabe, Preparation and luminescent properties of $Eu^{2+}$-activated glass ceramic phosphor precipitated with β-$Ca_2SiO_4$ and $Ca_3Si_2O_7$ Physica Status, Solidi A Appl. Res. 206 (2009) 919–922, https://doi.org/10.1002/pssa.200881326.
[10] N. Ojha, H. Nguyen, T. Laihinen, T. Salminen, M. Lastusaari, L. Petit, Decomposition of persistent luminescent microparticles in corrosive phosphate glass melt, Corrosion Sci. 135 (2018) 207–214.
[11] N. Ojha, T. Laihinen, T. Salminen, M. Lastusaari, L. Petit, Influence of the phosphate glass melt on the corrosion of functional particles occurring during the preparation of glass-ceramics, Ceram. Int. 44 (2018) 11807–11811.
[12] N. Garcia Arango, S. Vuori, H. Byron, D. Van der Heggen, P.F. Smet, M. Lastusaari, L. Petit, Near-infrared rechargeable glass-based composite with green persistent luminescence from new $Yb^{3+}$, $Tm^{3+}$ co-doped oxyfluorophosphate glasses, J. Alloys Compd. 927 (2022), 167048.
[13] L. Hu, P. Wang, M. Zhao, L. Liu, L. Zhou, B. Li, F.H. Albaqami, A.M. El-Toni, X. Li, Y. Xie, X. Sun, F. Zhang, Near-infrared rechargeable "optical battery" implant for irradiation-free photodynamic therapy, Biomaterials 163 (2018) 154–162, https://doi.org/10.1016/j.biomaterials.2018.02.029.
[14] Y. Wang, J. Ohwaki, New transparent vitroceramics codoped with $Er^{3+}$ and $Yb^{3+}$ for efficient frequency upconversion, Appl. Phys. Lett. 63 (1993) 3268–3270, https://doi.org/10.1063/1.110170.
[15] F. Auzel, Upconversion processes in coupled ion systems, J. Lumin. 45 (1990) 341–345, https://doi.org/10.1016/0022-2313(90)90189-I.
[16] H. Guo, Z. Li, H. Qian, Y. Hu, I.N. Muhammad, Seed-mediated synthesis of $NaYF_4$:Yb, Er/$NaGdF_4$ nanocrystals with improved upconversion fluorescence and MR relaxivity, Nanotechnology 21 (12) (2010), 125602, https://doi.org/10.1088/0957-4484/21/12/125602.
[17] G. Chen, T.Y. Ohulchanskyy, R. Kumar, H. Ågren, P.N. Prasad, Ultrasmall monodisperse $NaYF_4$:$Yb^{3+}$/$Tm^{3+}$ nanocrystals with enhanced near-infrared to near-infrared upconversion photoluminescence, ACS Nano 4 (2010) 3163–3168, https://doi.org/10.1021/nn100457j.
[18] H. Nguyen, M. Tuomisto, J. Oksa, T. Salminen, M. Lastusaari, L. Petit, Upconversion in low rare-earth concentrated phosphate glasses using direct $NaYF_4$:$Er^{3+}$, $Yb^{3+}$ nanoparticles doping, Scripta Mater. 139 (2017) 130–133, https://doi.org/10.1016/j.scriptamat.2017.06.050.
[19] T. Laihinen, M. Lastusaari, L. Pihlgren, L.C.V. Rodrigues, J. Hölsä, Thermal behaviour of the $NaYF_4$:$Yb^{3+}$,$R^{3+}$ materials, J. Therm. Anal. Calorim. 121 (2015) 37–43, https://doi.org/10.1007/s10973-015-4609-x.
[20] M.J. Treadaway, R.C. Powell, Luminescence of calcium tungstate crystals, J. Chem. Phys. 61 (1974) 4003–4011, https://doi.org/10.1063/1.1681693.
[21] Z. Piskuła, K. Staninski, S. Lis, Luminescence properties of $Tm^{3+}$/$Yb^{3+}$, $Er^{3+}$/$Yb^{3+}$ and $Ho^{3+}$/$Yb^{3+}$ activated calcium tungstate, J. Rare Earths 29 (2011) 1166–1169, https://doi.org/10.1016/S1002-0721(10)60618-7.
[22] X. Cheng, C. Yuan, L. Su, Y. Wang, X. Zhu, Effects of pressure on the emission of $CaWO_4$:$Eu^{3+}$ phosphor, Opt. Mater. 37 (2014) 214–217, https://doi.org/10.1016/j.optmat.2014.05.030.
[23] F. Yang, Y. Liang, M. Liu, X. Li, N. Wang, Z. Xia, Enhanced red-emitting by charge compensation in $Eu^{3+}$-activated $Ca_2BO_3Cl$ phosphors, Ceram. Int. 38 (2012) 6197–6201, https://doi.org/10.1016/j.ceramint.2012.04.071.
[24] R.D. Shannon, Revised effective ionic radii and systematic studies of interatomic distances in halides and chalcogenides, Acta Crystallogr. A. 32 (1976) 751–767, https://doi.org/10.1107/S0567739476001551.
[25] P. Kaur, A. Khanna, M.N. Singh, A.K. Sinha, Structural and optical characterization of Eu and Dy doped $CaWO_4$ nanoparticles for white light emission, J. Alloys Compd. 834 (2020), 154804, https://doi.org/10.1016/j.jallcom.2020.154804.
[26] Y.L. Xu, Y.L. Wang, L.S. Shi, X. Tan, Blue upconversion luminescence in $Tm^{3+}$/$Yb^{3+}$ codoped $CaWO_4$ polycrystals, Chin. Phys. Lett. 30 (8) (2013), 084207, https://doi.org/10.1088/0256-307X/30/8/084207.
[27] K. Van den Eeckhout, P.F. Smet, D. Poelman, Persistent luminescence in $Eu^{2+}$-doped compounds: a review, Materials 3 (2010) 2536–2566, https://doi.org/10.3390/ma3042536.
[28] V. Vitola, D. Millers, I. Bite, K. Smits, A. Spustaka, Recent progress in understanding the persistent luminescence in $SrAl_2O_4$:Eu,Dy, Mater, Sci. Technol. 35 (2019) 1661–1677, https://doi.org/10.1080/02670836.2019.1649802.
[29] A. Lukowiak, M. Stefanski, M. Ferrari, W. Strek, Nanocrystalline lanthanide tetraphosphates: energy transfer processes in samples co-doped with $Pr^{3+}$/$Yb^{3+}$ and $Tm^{3+}$/$Yb^{3+}$, Opt. Mater. 74 (2017) 159–165, https://doi.org/10.1016/j.optmat.2017.03.025.
[30] Deutsche Norm, Phosphorescent Pigments and Products – Part 1: Measurement and Marking at the Producer, 2009. DIN 67510–1:2009–11.
[31] A.J.J. Bos, R.M. van Duijvenvoorde, E. van der Kolk, W. Drozdowski, P. Dorenbos, Thermoluminescence excitation spectroscopy: a versatile technique to study persistent luminescence phosphors, J. Lumin. 131 (2011) 1465–1471, https://doi.org/10.1016/j.jlumin.2011.03.033.
[32] P. Zeng, X. Wei, M. Yin, Y. Chen, Investigation of the long afterglow mechanism in $SrAl_2O_4$:$Eu^{2+}$/$Dy^{3+}$ by optically stimulated luminescence and thermoluminescence, J. Lumin. 199 (2018) 400–406, https://doi.org/10.1016/j.jlumin.2018.03.088.